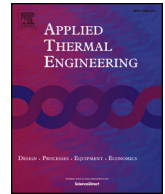




ELSEVIER

Contents lists available at ScienceDirect

Applied Thermal Engineering

journal homepage: www.elsevier.com/locate/apthermeng

Research Paper

Investigation on the contaminant distribution with improved ventilation system in hospital isolation rooms: Effect of supply and exhaust air diffuser configurations

Jinkyun Cho

Energy & Environment Business Division, KCL (Korea Conformity Laboratories), Jincheon 27872, South Korea

HIGHLIGHTS

- Expected risk of infection from patients to healthcare workers in an AIIR was found.
- We investigated how to remove airborne contamination effectively in AIIRs.
- Both full-scale field experiments and CFD simulations were performed.
- Transport of gaseous pollutants is indicated by tracer gas.
- By changing the exhaust air flow, the exposure pollutant level was significantly reduced.

ARTICLE INFO

Keywords:

Airborne infectious isolation room
Contaminant distribution
Ventilation system
Full-scale field experiment
CFD simulation
Tracer gas containment testing

ABSTRACT

This study, that is practice-based learning in a real hospital construction project, has evaluated the ventilation performance of three strategies in the protection of health care workers and HVAC control for airborne infectious diseases induced by contaminated exhaled air from patients in a negative pressure isolation room. This paper examines air flow path and airborne pollutant distribution by computational fluid dynamics modeling and field measurement. In hospitals, the risk of virus diffusion mainly depends on air flow behavior and changes in direction caused by supply air and exhaust air locations. An improved isolation room ventilation strategy has been suggested, and is found to be the most efficient in removing contaminants based on the observations and simulation results from three ventilation systems. The results show that ventilation systems utilizing the “low-level extraction” technique are very effective at removing pollutants in the human breathing zone. A new clean isolation room ventilation strategy has been developed that employs two exhaust air grilles on the wall behind the bed at low floor level, coupled with a fan filter unit, and is found to have the highest pollutant removal efficiency.

1. Introduction

Airborne transmission is one of the main spread routes for a number of infectious diseases such as smallpox, tuberculosis [1]. New diseases and outbreaks are always a threat. More than 8000 reported cases of Severe Acute Respiratory Syndrome (SARS) resulted in 774 deaths and led to a wave of research and standardization of medical facilities with respect to airborne diseases. 36 patients died and 186 people were infected during the outbreak of Middle East Respiratory Syndrome (MERS) in South Korea in May 2015 [2]. Outbreaks of such airborne diseases in hospitals elevate the risk of infection from patients to healthcare workers (HCWs) and other patients. Due mainly to contact with an infected host, also poor ventilation in hospitals, MERS viruses

began to spread rapidly to patients, visitors, and even to HCWs [3]. Isolation is the primary control. Systems serving airborne infectious isolation rooms (AIIR), highly contaminated areas, should maintain a negative air pressure with respect to adjoining rooms or corridors. Because airborne transmission of pollutant has a possibility of disease spread to HCWs and patients, HVAC systems are a secondary control measure. The plan of AIIR with negative pressure includes a complex process of decisions. The specifications of mechanical ventilation system, location, layout, interior finishing, and AIIR facilities are critical to the design concepts [4]. Because of return air (RA), exhaust air (EA) and supply air (SA) locations, the risk of virus dispersal at the hospital is influenced by changes in movement and direction of air flow [5–7].

E-mail address: maxjcho@yonsei.ac.kr.

<https://doi.org/10.1016/j.applthermaleng.2018.11.023>

Received 3 July 2018; Received in revised form 13 October 2018; Accepted 7 November 2018

Available online 07 November 2018

1359-4311/ © 2018 Elsevier Ltd. All rights reserved.

Nomenclature		OA	outside air
HCW	healthcare workers	FFU	fan filter unit
AIIR	airborne infectious isolation room	CAV	constant air volume
RA	return air	MERV	minimum efficiency reporting value
EA	exhaust air	HEPA	high efficiency particulate air
SA	supply air	ULPA	ultra low penetration air
		CFD	computational fluid dynamics

Major studies analyzing how airborne viruses spread have also been carried out on surgery rooms and isolation rooms, focusing on the diffusion analysis of viral pathogens. (Rice et al. [8]; Bjorn and Nielsen [9]; Huang and Tsao [10]; Qian et al. [11]; Rui et al. [12], Morawska [13], Li et al. [14], and Yu et al. [15] used a tracer gas simulation to analyze the infection path in hospitals where the outbreak occurred, and confirmed by examining the tracer gas concentration in the space between the first infected patient and those infected afterwards that the virus had indeed spread through the air. Studies on the spread of viral pathogens and contaminants generally assume that the breathed air exhaled from patients is the source of contaminants or pathogens and their diffusion is therefore analyzed. Considering the breathed air, Hayashi et al. [16] reported that the breathing volume of an adult under normal conditions was 6L/min based on 0.7 met of activity during sleep (convective heat transfer 33.3 W/person), and the volume of exhaled air under normal conditions was 14.4 L/min. Abraham et al. [17] used the large-eddy simulation (LES) method in an operation room (OR) and validated the model with fog flow visualization. It shows the value of such validation and the appropriate use of CFD. Shirozu et al. [18] used RANS-based turbulence models and validated by experiment. These papers showed the critical importance of validation and also the power of CFD to carry out simulations. In particular, calculations were performed without moving surgeons and staff but the experiments were performed with a moving surgical team. The results of that case were not adversely affected.

In this study, air flow pattern, air velocity and pollutant distribution were investigated using numerical simulations of molecular diffusion, and removal of pollutants inside a negative pressure AIIR equipped with three ventilation strategies were analyzed based on EA locations. Field measurements were conducted in an AIIR with advanced ventilation. The results of CFD numerical analysis were validated by the field measurement results. This has been done to make sure that predictions of pollutant concentrations and air flow in succeeding cases to other systems are reliable and accurate. Finally, airflow and pollutant concentration profiles with FFU were simulated and analyzed for these proposed strategies to develop an optimum design for removing pollutant from this negative pressure AIIR and provide better protection for the HCWs. This research is practice-based learning in a real hospital construction project. A series of full-scale field measurements and CFD modeling were carried out in the new AIIR of the Hospital. The aim of this study is to examine the ventilation performance relationships between HVAC system and AIIR architectural design in hospital building projects. The research methodology and procedures are shown in Fig. 1.

2. Negative pressure AIIR design

As shown in Table 1, negative pressure AIIR design varies from country to country. AIIRs are designed the single pass approach to bring clean air from the clean zone to the contaminated zone. According to the US ASHRAE-170 standard [19], the pressure difference required maintaining negative pressure is minimum 2.5 Pa. The actual negative pressure level will depend on several factors: differences in the SA and EA volume; air flow paths; and air flow openings and physical configuration of the wardroom. To maintain negative pressure in a wardroom, the EA volume needs to be 10% larger than the SA volume [20]. For a room with low airtightness, the HVAC system may not be able to

provide the necessary EA/SA air flow differentials.

AIIRs in existing healthcare facilities needs to achieve at least 6 air changes per hour (ACH) in order to reduce the concentration of pollutants. Because dilution strategy is improper for particulate contaminants, air mixing should not be encouraged. From the SA is either appropriately conditioned air from outside of the building or re-circulated air from the central AHU, the EA, contaminated air in the AIIR, is extracted to the outside via the single pass. In new construction of healthcare facilities, the air change rate of AIIR should be at least 12 ACH [19,21,22]. The problem of AIIR ventilation systems can be identified, such as air mixing and inappropriate directional air flow pattern. Ideally, the clean SA should be introduced near HCWs and then, EA should be removed near the patients [23]. The typical AIIR ventilation strategy employs a ceiling SA and ceiling EA system and/or optional air recirculation unit with HEPA filter such as FFU. As shown in Fig. 2(a), this ventilation strategy may not efficiently reduce the pollutant concentrations of an infectious source at specific locations due to air mixing in the AIIR. In short, SA is in flowed near staff, but EA is not captured near patient. There will be an expected high risk of infection from patients to HCWs caused by air mixing in an AIIR. An improved ventilation system in Fig. 2(b) as the best arrangement is to EA grilles on the wall near the floor at the head of the bed, and to SA diffusers at the ceiling above the foot of the bed. The bottom of the EA grilles should be located about 150 mm above the floor. This ventilation strategy has been adopted in some hospitals, but the area in front of the EA grilles is often not kept clear of obstructions such as supply carts and furniture. Because the location of the SA and EA is very important, two wall-mounted EA grilles coupling with FFU was developed for effective removal of airborne contamination. (Fig. 3) The overall goal of this

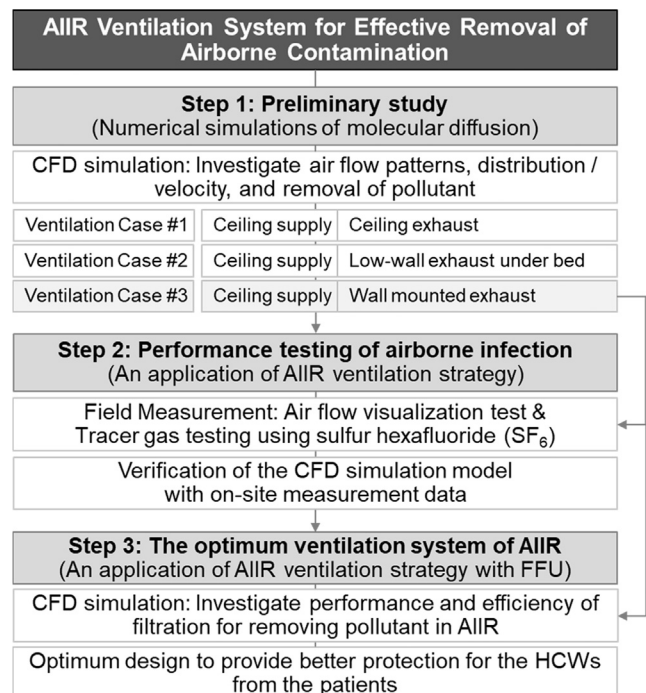


Fig. 1. Research methodology and procedure.

Table 1
Design standards for AIIR to prevent airborne contamination.

	Organization	Air Change Rate (ACH)	Pressure differential	Recirculation	Anteroom
USA	Center for disease control and Prevention	Existing	New/remodeling	More than 2.5 Pa	Yes (w/HEPA filter)
		More than 6	More than 12		
Canada	Public Health Agency of Canada	Existing	New/remodeling	–	Yes (w/HEPA filter)
		More than 6	More than 9		
UK	Department of Health	More than 10		More than 5 Pa	No
Norway	Folkehelseinstitutt	More than 12		More than 5 Pa	No
Australia	Department of Health & Human Services	Mandatory	Recommend	More than 15 Pa	No
		More than 12	More than 15		
Hong Kong	Infection Control Committee Department of Health	Existing	New/remodeling	More than 2.5 Pa	Yes (w/HEPA filter)
		More than 6	More than 12		
Korea	Center for Disease Control and Prevention	Mandatory	Recommend	More than 2.5 Pa	Yes (w/HEPA filter)
		More than 6	More than 12		

study is to find an improved ventilation system based on contaminant concentrations which are the modeled and measured parameter and best design practices should be followed.

3. Numerical simulation for AIIR ventilation strategies

3.1. Numerical simulation procedure

The spread of the airborne contamination was analyzed according to the types and location of the supply air diffuser and exhaust air diffuser in the isolation rooms to propose designs to reduce the airborne transmission by utilizing CFD simulation, which can thoroughly analyze the spatial airflow and the spread of the contamination. To investigate the dynamics of the ventilation flow and the airborne contamination in the conditions of coughing and breathing of a patient was performed on the three CFD model. The AIIR in Fig. 4 shows the locations of the HCWs, patient, door to the bathroom, door to the anteroom, and SA and EA openings for the various cases analyzed in this study. This investigation sought to use the thermo-fluid boundary conditions for several types of indoor airflow with STAR-CCM+. The renormalization group *k-ε* was selected as the turbulence model with multi-component gas fluid (Air/SF₆), while SIMPLE was used as the pressure-velocity coupling algorithm. 550,000 grid cells were arrayed across the simulation domain.

3.1.1. Boundary conditions

The room has roughly 16 m² floor space and 2.6 m ceiling height, with a drop ceiling in part of the room. The sensible heat load due to four occupants (patient and 3 HCWs) was assumed to be 248 W, whereas the sensible heat load due to the lighting was assumed to be 11.9 W/m². The room has an east facing window with a solar heat gain of 30 W/m². All other exterior walls of the room are assumed to be adiabatic. Thus, the total sensible load in the AIIR is assumed to be 56.8 W/m². The total SA volume and the temperature were specified at 500 m³/h (12 ACH) and 16.4 °C, respectively. The two square diffusers

placed on the drop ceiling are designed to SA 250 m³/h. The EA flow rate from the room was designed to maintain 400 m³/h, whereas the bathroom EA flow rate was designed 200 m³/h. Thus, the total EA flow rate was assumed to be 600 m³/h with a deficit of 100 m³/h, which was supplied through the leakage under the main door from the anteroom. The AIIR was assumed to control under negative pressure and all doors were closed. Boundary conditions and geometries are summarized in Table 2.

3.1.2. Working fluid

The sulfur hexafluoride (SF₆) gas was used as the working fluid. In the case of solid particles, such as dust or microbes, the analysis is possible in the network model because it has a pollution source model for solids, but the analyses in the CFD model handles the solid particle diffusion indirectly by setting gases such as CO₂, N₂O, or SF₆ as the tracer gas and inputting their gaseous physical properties. The unique properties of SF₆ have led to its adoption for a number of industrial and scientific applications including tracer gas for studying airflow in ventilation systems. Researches on the diffusion of such pathogens as viruses or pollution sources generally assume discharged air from breathing to be the source of the pollution or pathogen and then analyze its diffusion. We first obtained the steady state solutions for the air flow field, and then tracer gas was continuously released into the AIIR through the source manikin’s mouth in bed at a mass fraction of 0.04 [24], with an upward exhalation velocity of 0.955 m/s. The height of source location (mouth of patient) is 0.9 m above the floor.

3.1.3. Alternative model generation

The possible flow paths of airborne contaminants are analyzed by tracing the air flow path ways emitted from the face of patient. This analysis focuses upon low-momentum pathogen releases (i.e., does not focus on high momentum releases such as full-volume coughing) and assumes most of the airborne pathogens emitted from the face of patient would follow the flow path of the air, neglecting any settling and deposition of these particles on the surfaces. A total of three cases

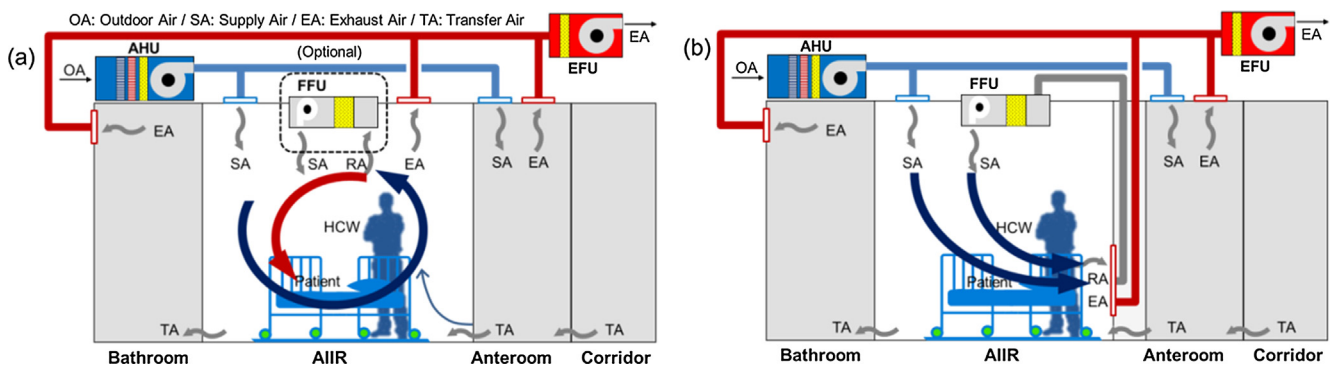


Fig. 2. Ventilation strategies of the AIIR; (a) typical ventilation system and (b) improved ventilation system.

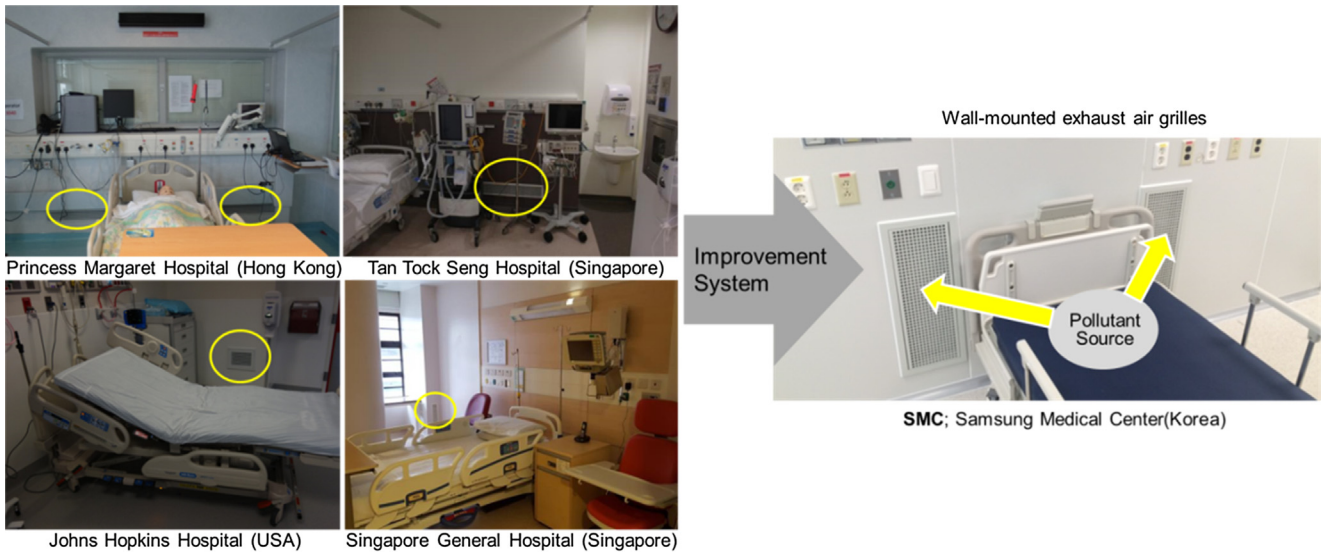


Fig. 3. Determining the better location of EA grilles for AIIR ventilation system.

analyzed for various locations of EA grilles are described below and in Table 3.

- Case#1: Ceiling SA diffusers over left side of patient’s head and ceiling EA grilles near the toilet door. This is a typical HVAC configuration for a negative AIIR (Fig. 4(a)).
- Case#2: Ceiling SA diffusers over left side of patient’s head and the ceiling exhaust replaced with the low wall horizontal EA grille placed under the patient’s bed at 0.2 m above the floor (Fig. 4(b)).
- Case#3: Ceiling SA diffusers over left side of patient’s head and the ceiling exhaust replaced by two wall mounted EA grilles placed behind the patient’s head at 0.2 m above the floor (Fig. 4(c)).

In subsequent chapter, airflow patterns from the CFD (vectors/streamlines) were compared with experiments. Instantaneous vector

patterns/streamlines are useful for flow determination. [17] In the related research [18] results, CFD simulation without moving healthcare staffs and experiment with moving healthcare staffs was not adversely affected. Therefore, numerical simulations were performed without moving HCWs.

3.2. Numerical simulation results

Computational results for each case are presented in the form of color contour plots showing pollution distribution and vector plot. They show the probable path of contamination released from the patient and the air flow distribution in AIIR. Fig. 5 shows concentration distribution patterns at a 1.4 m horizontal plane representing the respiration level of the HCWs during treating the patient. The concentration of pollutants is reduced as they move away from the patient. The stagnation of air was

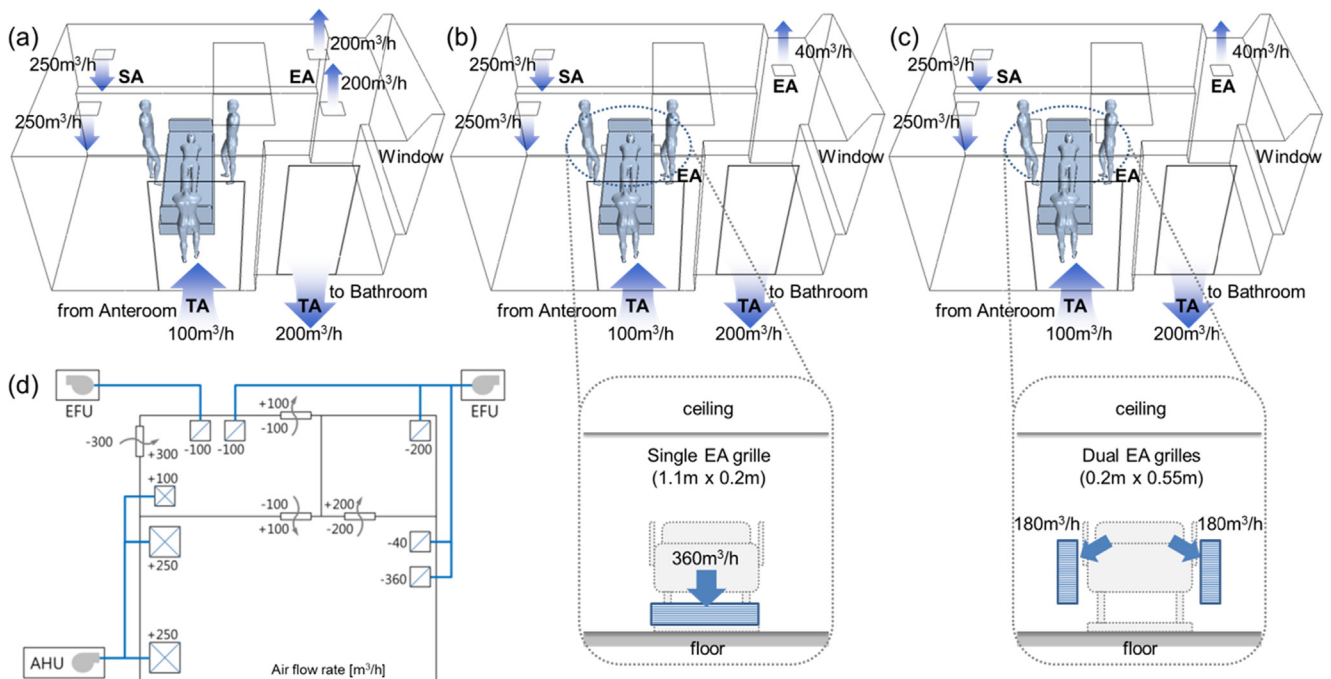


Fig. 4. CFD modeling for ventilation strategies; (a) ventilation Case#1, (b) ventilation Case#2, (c) ventilation Case#3 and (d) air flow diagram of the AIIR and surroundings.

Table 2
Boundary conditions with default air change rates.

Turbulence model	Standard <i>k-ε</i> model (wall function used)
Supply in AIIR	Physical specifications: see Fig. 4 Airflow rate: see Table 3 Default supply velocity $V_{in} = 0.772$ m/s (500 m ³ /h) $T_{in} = 16.4$ °C
Transfer from anteroom	Physical specifications: see Fig. 4 Airflow rate: 100 m ³ /h $V_a = 0.411$ m/s $T_a = 26.0$ °C
Transfer to bathroom	Physical specifications: see Fig. 4 Airflow rate: 200 m ³ /h $V_b = 0.902$ m/s $T_b = 26.0$ °C
Exhaust from AIIR	Physical specifications: see Fig. 4 Airflow rate: see Table 3 k_{out} , ϵ_{out} , T_{out} = free slip
Lying manikins	Uniform heat flux: 62 W no slip boundary
Mouth of source manikin in AIIR	Exhalation velocity: 0.955 m/s, mass fraction of gas(SF ₆): 0.04 $T_m = 30$ °C (i.e. gas(SF ₆) release rate: 0.54 m ³ /h).
Walls	2 and 1 W/m ² at ceiling/floor no slip boundary standard wall function
Bedside Grid cells	Adiabatic wall boundary condition 550,000

observed in some regions with the high concentration of pollutant. It was observed that there is air short circuiting between the SA diffusers and the EA grilles from the vector plot of air velocity. In the AIIR, the CFD simulation used to predict pollutant distribution profiles and air flow pattern was well analyzed. The absolute concentration value of pollutant has no significance in this research. Rather, it is the relative concentration profile between one ventilation system and the other that is very important. Table 4 shows the exposure level of pollutant to the HCWs. Ventilation Case#1 has high concentration values that ranging between 33.1 and 72.7 ppm. The lowest concentration is observed around HCW-3, while the highest concentration is observed at HCW-1. While giving treatment to the patient, the HCW will likely be standing at 1.4 m with the higher exposure level of pollutant.

It indicates that Case#1 is poor for removing pollutants from the AIIR. Compared with Ventilation Case#1, Ventilation Case#2 and Case#3 have lower concentration values, ranging between 25.1 and 34.4 ppm, and between 21.2 and 24.4 ppm, respectively. Table 5 shows the percentage difference of predicted concentration between the ventilation Case#1, Case#2 and Case#3. When the HCWs were treating the patient, there was a large difference in the pollutant exposure level. At 1.4 m location average value of pollutant concentration, Case#2 was 11.9% lower than in Case#1. Similarly, Case#3 was more effective in removing contaminant in the AIIR compared to Case#1 and Case#2 with 24.2% and 14.0% respectively. For the average concentration of whole room, Case#2 was lower than Case#1 with 22.7%. Exposure

Table 3
Boundary conditions of EA for ventilation cases.

	Exhaust Air (Default extract velocity V_e)			
	Total	Ceiling	Wall-mount (under bed)	Wall-mount (behind bed)
Case #1 (Base)	400 m ³ /h	400 m ³ /h, $V_{out} = 0.617$ m/s (0.3 m × 0.3 m) 2EA	–	–
Case #2	–	40 m ³ /h, $V_{out} = 0.123$ m/s (0.3 m × 0.3 m) 1EA	360 m ³ /h, $V_{out} = 0.455$ m/s (1.1 m × 0.2 m) 1EA	–
Case #3	–	40 m ³ /h, $V_{out} = 0.123$ m/s (0.3 m × 0.3 m) 1EA	–	360 m ³ /h, $V_{out} = 0.455$ m/s(0.2 m × 0.55 m) 2EA

level of Case#3, 34.8 ppm, was lower compared to Case#1 (48.4 ppm) and Case#2 (37.4 ppm). Ventilation case #3, which was the best of three cases to remove pollutant from AIIR, bound to improve efficiency with 28.1% of Case#1 and 7.0% of Case#2. A clean air moves from the HCWs to the patient resulted in the improved air flow pattern in healthcare facilities. The use of a single pass setup is expected to lower the risk of infection from patients to HCWs These results indicated that placement of EA grilles directly behind the patient’s head can potentially provide a ready flow path for airborne contamination to exit the AIIR without remarkable recirculation and entrainment back into the SA stream. A combination of locations for and types of SA diffusers, locations of room EA and SA flow rates can affect the air flow patterns in the AIIR which are quite complex and specific to a particular design configuration. The air flow profile at the patient’s bed is less than 0.25 m/s within the recommended threshold air velocity value.

4. Full-scale field measurement

4.1. Experimental procedure

The results of tracer gas experiments help to understand the possible spread of airborne pollution sources for example in “S” medical center (in Korea), which were vulnerable in the MERS in 2015. This medical center decided to permit ventilation Case#3 for negative pressure AIIRs in 2016 according to the results of the preliminary ventilation strategies study. A series of full-scale field measurements were conducted. Field measurement methods used to analyze data can be classified into two categories as smoke testing and tracer gas containment testing.

4.1.1. The AIIR with ventilation Case#3

This research was carried out in a negative pressure AIIR on the second floor of an unoccupied 3-story isolation unit extension before the official opening. The new isolation unit had 6 negative pressure AIIRs and two intensive care units (ICU). The second floor consists of a corridor with four AIIRs. Each floor of the isolation unit has a separate constant air volume (CAV) ventilation system that provides 100% outside air (OA). Filtration was achieved using minimum efficiency reporting value (MERV) 8 panel filters. [25,26] As shown in Fig. 6(a), The anteroom was maintained at a pressure – 2.6 Pa with respect to the corridor when the door between the corridor and anteroom was closed. Likewise, a correctly functioning AIIR was maintained at a pressure – 3.8 Pa in respect of the anteroom when the AIIR-anteroom door was closed. Every two AIIRs have their own toilet but use a shared anteroom. Air in the AIIR was exhausted through the bathroom’s fan. There were two ceiling SA diffusers and one ceiling EA grille and two wall EA grilles placed behind the patient’s head at 0.2 m above the floor level. The total air change rate of the AIIR is 12 ACH.

4.1.2. Contaminant source mock-up

In these experiments, SF₆, same working fluid in CFD analysis, was used as tracer gas. SF₆ injection rate is regulated via a mass flow controller and SF₆ was continuously released from a cylinder as a point emitting tracer gas at 1.09 L/min. Fig. 6 shows the locations of sampling

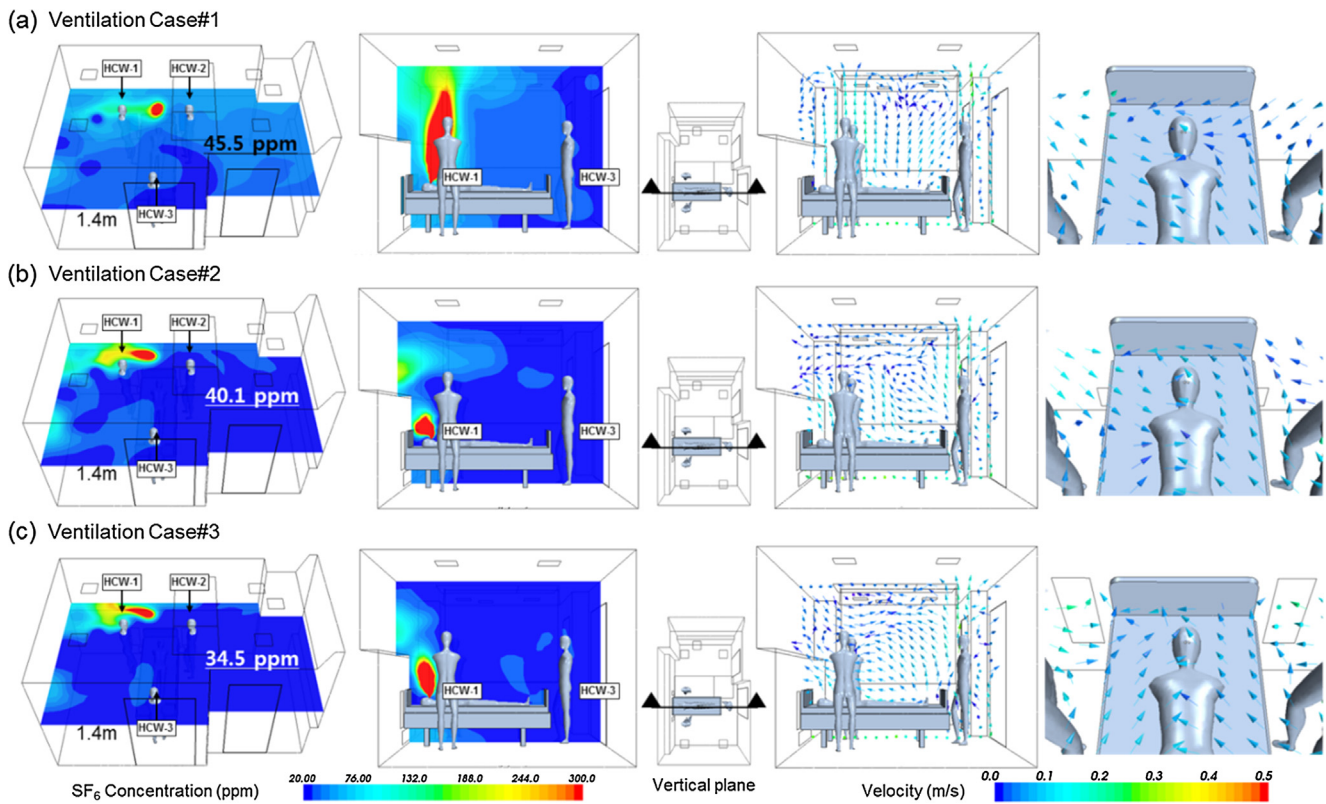


Fig. 5. Simulation results of concentration profile of SF₆ and velocity vector plot; (a) Ventilation Case#1, (b) Ventilation Case#2 and (c) Ventilation Case#3.

Table 4

The pollutant's exposure level of the HCWs.

	Mean SF ₆ concentration (ppm)		
	Ventilation Case #1	Ventilation Case #2	Ventilation Case #3
HCW-1 (1.4 m)	72.7	34.4	24.4
HCW-2 (1.4 m)	40.0	27.6	21.2
HCW-3 (1.4 m)	33.1	25.1	21.3
Average of 1.4 m level	45.5	40.1	34.5
Average of Room	48.4	37.4	34.8

Table 5

The pollutant concentration percentage difference of 3 ventilation cases.

Percentage difference	SF ₆ concentration percentage difference (%)					
	Ventilation Case #1 (C _{v1})		Ventilation Case #2 (C _{v2})		Ventilation Case #3 (C _{v3})	
	Base	(C _{v1} -C _{v2})/C _{v2}	Base	(C _{v2} -C _{v1})/C _{v1}	Base	(C _{v3} -C _{v1})/C _{v1}
HCW-1	0.0	34.4	-52.7	0.0	-66.4	-29.1
HCW-2	0.0	44.9	-31.0	0.0	-47.0	-23.2
HCW-3	0.0	31.9	-24.2	0.0	-35.6	-15.1
Average of 1.4 m level	0.0	13.5	-11.9	0.0	-24.2	-14.0
Average of Room	0.0	29.4	-22.7	0.0	-28.1	-7.0

and injection in the AIIR. At a constant rate of tracer gas, SF₆ was injected near a patient's bed at 0.9 m above floor. A tracer gas analyzer continuously measured at six sampling locations for the concentration

of SF₆.

4.1.3. Measurements of contaminant

To evaluate the pollutant exposure level of the HCW, three points (SP-1, SP-2 and SP-3) were located near the bed at 1.4 m from the floor. These measuring points were selected, as HCW will be standing at these points while treating the patient. Two sampling points (SP-4 and SP-5) were located at the two EA grilles to evaluate for removing pollutants in the room. And one sampling point (SP-6) was in the anteroom.

4.1.4. Measuring instruments accuracy

The volumetric flow rates were measured by multi-gas sampler & doser and photoacoustic multi-gas monitor. Accuracy is the degree to which the measured value agrees with the true value. The accuracy of measuring instruments was assessed through calibration. Uncertainties of field measurement were evaluated by CFD simulation verification.

4.2. Measurement results

Smoke testing was used to visualize the air movement directions in the AIIR and to evaluate how well pollutants are removed. Fig. 7(a) shows the results of a smoke test conducted in a negative pressure AIIR, visualizing air flow by using a portable fog generator. Results showed that the indoor air did not mix or spread inside of the AIIR, but was discharged immediately through two low wall EA grilles placed behind the patient's head. Fig. 7(b) illustrates the SF₆ concentration profiles at the six monitoring points in the AIIR. As SF₆ was injected, the tracer gas concentration increased rapidly at monitoring locations SP-1 to SP-5. It was observed that the concentration trend at each point reached equilibrium after 20 min and showed a similar profile. Monitoring location SP-6 shows only trace levels for concentration of SF₆. This means that there was no air flow from the AIIR to the anteroom when the door was closed and the AIIR was under negative pressure. At SP-4 and SP-5, the two EA grilles, the SF₆ concentration continued to maintain at a

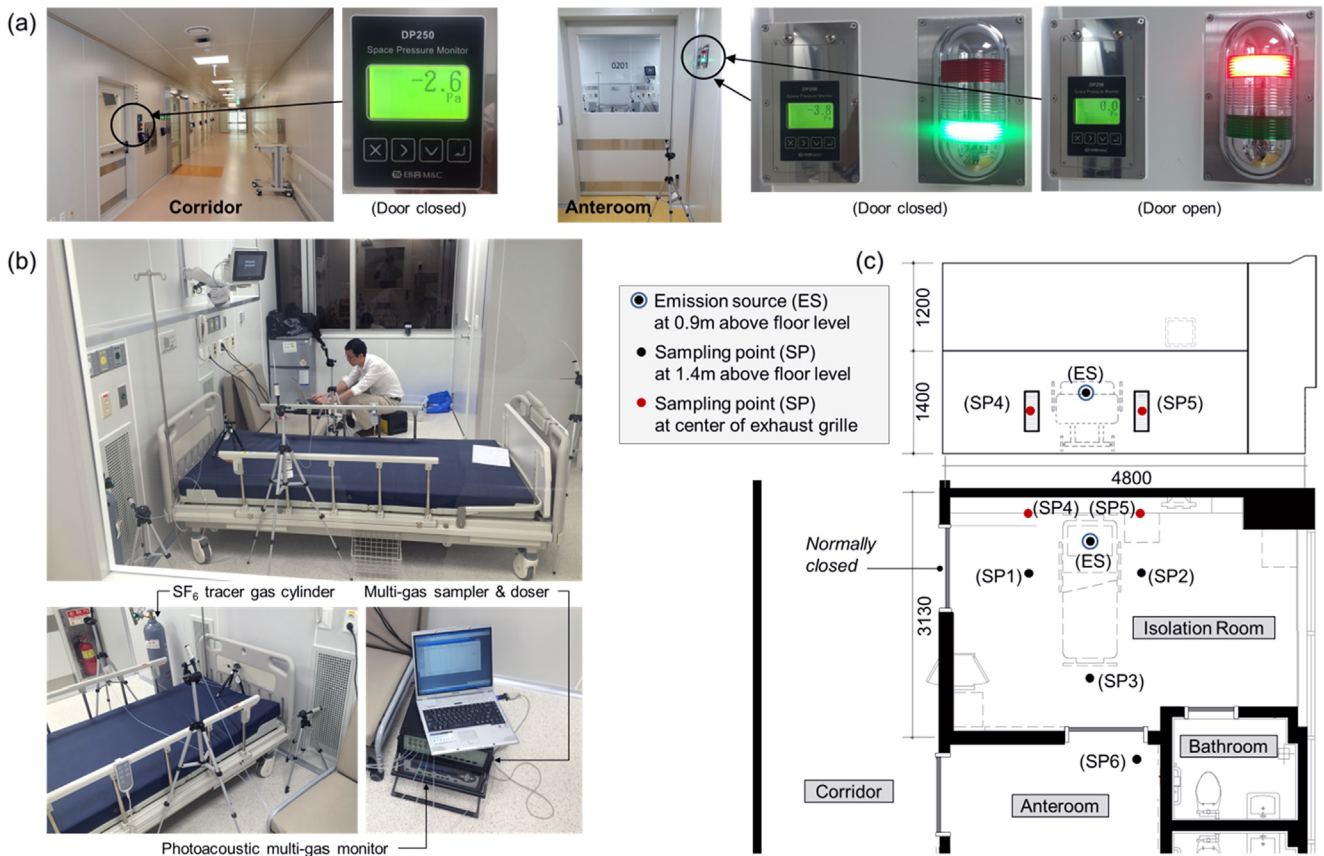


Fig. 6. (a) Pressure differential between rooms, (b) field test room and measurement instruments and (c) position of sampling points in the AIIR.

higher than the other three monitoring locations over the period of measurement. The SF₆ concentration of SP-4 and SP-5, have dynamic range of pollution concentration, also increased at a faster rate as compared to those concentration at the other locations. Average pollution concentration on SP-4 and SP-5 is 46.2 ppm and 47.1 ppm respectively. This was over 2.2–3.3 times higher than on SP-1(21.5 ppm), SP-2(17.8 ppm), and SP-3(14.4 ppm). It is assumed that these average values were so small due to air flow movement caused by the large area of the EA grilles. Assuming maximum values, maximum pollution concentration on SP-4 and SP-5 is respectively 142 ppm and 132 ppm, which are over 4.2–5.8 times higher than on SP-1 to SP-3.

Consequently, it was determined that pollutants were removed with high efficacy.

4.3. Simulation verification

For verification of the CFD simulation, the AIIR with ventilation Case#3 (Fig. 3(c)) was compared with on-site measurement data. In the modeling of contaminant's migration patterns under steady-state condition, besides specifying the flow conditions across the boundaries, the neighboring rooms' conditions of the source term within the continuum and its boundaries must be defined. [27] Boundary conditions were

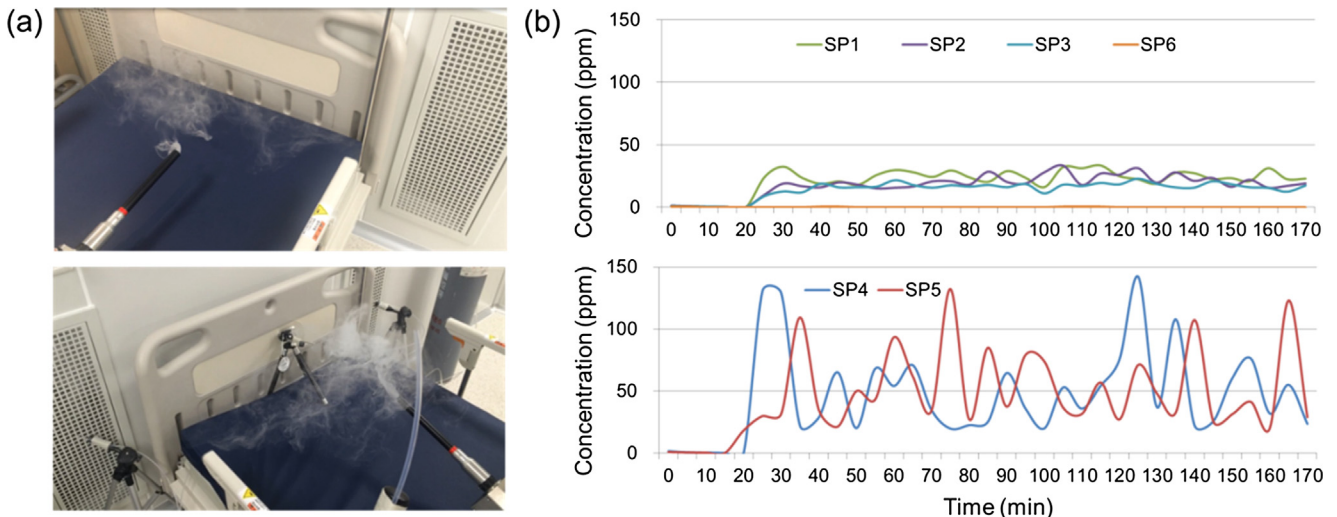


Fig. 7. Measurement results; (a) air flow visualization test in the AIIR and (b) SF₆ concentration profile at the monitoring points.

about the same for the ventilation Case#3 except total heat load and SA temperature. These analyses were carried out for partial load conditions which are more prevailing than the peak design load conditions. Because field measurement was carried out at night and there was almost no difference between indoor and OA temperature, the windows and exterior walls of the room were assumed to be adiabatic. The total sensible heat load was assumed to be 11.95 W/m² in consideration of artificial lighting only. The OA, with a total air exchange rate of 12 ACH, was supplied to the room at 24.6 °C. The release source was simulated at 1.09 L/min, as a point discharging SF₆. Fig. 8(a) shows the horizontal concentration distribution pattern of 1.4 m from the floor representing the HCWs' respiration level when attending to the patient. The dispersion of contaminants is not symmetrical, which is influenced by the indoor air flow pattern. As shown in Fig. 8(b), around the patient's breathing level at 0.9 m from the floor, it is clear that the highest pollutant concentration is found. The concentration of SF₆ is lower as they move away from the patient. Fig. 8(c) illustrates the predicted air flow pattern of a vertical section of the AIIR. The air flows towards the patient and is discharged via two EA grilles mounted on the wall and one ceiling EA grille in the room. The patient on the bed is experiencing about 0.10 m/s air flow. This velocity is the recommended value of less than 0.25 m/s. [28] As shown in Table 6, the measured concentration is correlates well with the predicted concentration at SP-1, SP-2 and SP-3 that are the breathing level of the HCW. The percentage difference between the simulation and measurement results ranged between -9.7 and 7.0. As shown in Fig. 9, the measured concentration of pollutant at SP-1 to SP-3 did not much change with a deviation of 4.3 ppm (Q1–Q3) during the experiment. This model is reasonably accurate to evaluate the profile of pollutant in the AIIR. Since the simulation results give concentration ranges similar to those of the measurements, we consider the simulation method to be primarily validated. Therefore, we used the same simulation method to carry out additional analysis. In the validation work, it should be noted that the multi-component gas type and emission rate of the source is 1.09 L/min. Before validation of the prediction results against the measurement results, the model was already modified representing the ventilation cases.

5. Discussion

Best practice includes design stage consideration of factors related to ventilation and isolation room performance. According to the results of field measurement and numeric analysis of three ventilation strategies of the AIIR, ventilation Case #3 was the most effective at removal of airborne contamination.

The system configuration concept and CFD model of the AIIR ventilation Case #3 with FFU is shown in Fig. 10. Boundary conditions and geometries are summarized in Table 7. For CFD simulation model, the AIIR with ventilation Case #3 was compared with the same ventilation system, an add-on FFU system. Boundary conditions were roughly the same for ventilation Case #3 in Section 3, except for the supply air and exhaust air flow rate change driven by the FFU system. The FFU style

Table 6

Corroboration of simulation and measurement results.

Sample point	Mean SF ₆ concentration (ppm)		Percentage difference (%)(C _s -C _m)/ C _m
	CFD simulation (C _s)	Field measurement (C _m)	
SP-1	23	21.5	7.0
SP-2	17	17.8	-4.7
SP-3	13	14.4	-9.7

isolation room is a method for cleaning a space by installing the FFU to achieve the required levels of sterility for HCWs. This is suitable for an AIIR requiring high sterility with single airflow and adopted widely to operating theaters in hospitals.

The ventilation Case #3 in addition to FFU can improve the performance of contaminant control when patients check out of and check into the AIIR. Most common bacteria are removed by the 0.3-micron pore size HEPA filters, rated 99.997% efficient at retaining particles. Fig. 11(a) shows the concentration distribution pattern of horizontal planes at 1.4 m and 0.9 m from the floor level to represent the breathing level of the HCWs while treating the patient. The high concentration found near the patient is clearly visible. However, the pollutant's concentration was not diluted and the stagnation of air was not observed in the AIIR. It was found that airborne contamination seemed to be perfectly removed by FFU. The greater flow rate of supply air already filtered by the FFU should pass over the patient and return directly to the exhaust grille in a single pass without entraining back into the supply airstream, which will ensure that it does not mix with the room air. The dispersion of pollutant is very efficiently removed, and this is influenced by directional airflow patterns of the FFU system in the room. As shown in Fig. 11(b), the predicted airflow profile of horizontal planes, the supply air was introduced near the HCWs, and the exhaust air was directly collected near patients. It shows the predicted airflow profile of a vertical plane along the length of the room. It is observed from the air velocity vector plot that there is no short-circuiting of air between the air diffuser and the exhaust grille. Table 8 shows the pollutant's exposure level of the HCWs. Ventilation Case #3 with FFU has very low concentration values ranging between 2.0 and 8.9 ppm. The percentage difference between Case #3 and Case #3 with FFU ranged between -58.0 and -90.6. At 1.4 m location average value of pollutant concentration, Case #3 with FFU was 85.2% lower compared to Case #3. For the average concentration of the whole room, Case #3 with FFU was much lower than the 79.6% in Case #3. This advanced ventilation strategy increased removal efficiency of airborne contamination remarkably. Advanced baffling technology ensures uniform airflow across the filter face and attenuates sound. Designers can select between HEPA filters, rated 99.97% efficient at removing particles ≥ 0.3 microns, or ULPA filters, rated 99.997% efficient at removing particles ≥ 0.12 microns. This ventilation system will provide year-round, 24/7 operation, depending on AIIR clean air quality.

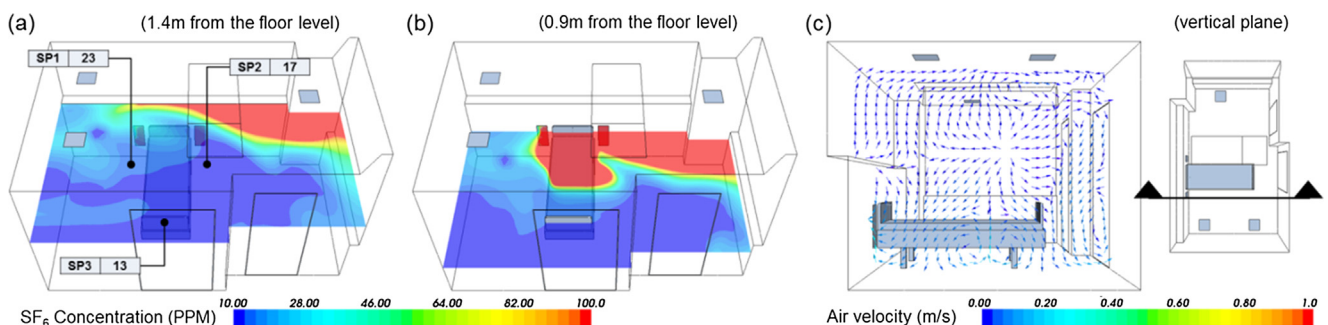


Fig. 8. CFD simulation verification results; (a), (b) concentration profile of SF₆ and (c) velocity vector plot.

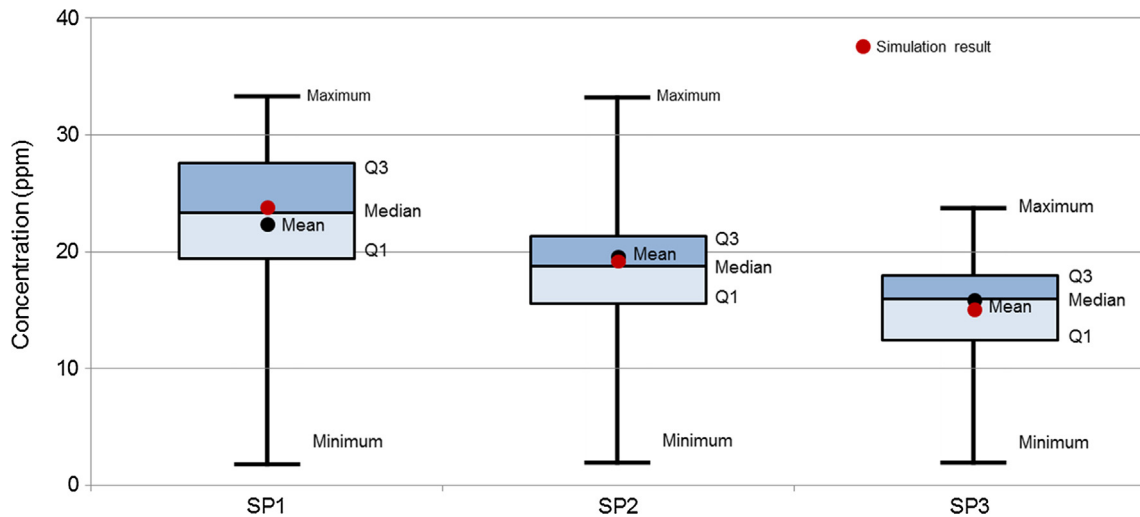


Fig. 9. Comparisons of onsite measurement results at SP-1 to SP-3.

6. Conclusions

This research has evaluated the performance of ventilation strategies and the HVAC controls of airborne contamination from patients in AIIRs of hospitals. This study has conducted to increase the understanding of the improved ventilation system, including both numerical simulation and full-scale experimental work. It demonstrates that the air flow paths, induced SA flow paths, and EA grille placement can be coordinated to establish effective contaminant control. Locations of the SA and EA openings are the most important elements that directly affect the pollutants dispersion in the room. Thus a careful evaluation of the HVAC configuration can help in gaining the insight and optimizing the flow path of air to obtain the desired combination of occupant thermal comfort and the best possible hygienic conditions in the AIIR. A combination of locations and EA/SA diffuser types, locations of the room RA, and EA/SA flow rates can affect the air flow patterns in the AIIR, which are very complex and specific to a particular design configuration. In this research, AIIR ventilation strategies for reducing the exposure level of pollutant have been developed. They are as follows:

- Arrange EA grilles and SA diffusers to allow clean SA to move from the clean area (HCW) to the contaminated area (patient), and exhausted from the AIIR. And ensure that the AIIR achieves at least 12 ACH for effective contaminant control.
- There was large difference in the pollutant exposure level to the

HCWs, when attending to the patient. At 1.4 m location average value of pollutant concentration, Case#2 (ceiling SA and low wall EA under the patient’s bed at 0.2 m above the floor) was 11.9% lower than in Case#1 (ceiling SA and ceiling EA). Similarly, Case#3 (ceiling SA and the two wall mounted EA behind the patient’s head) was more effective for removing pollutants in the room than Case#1 and Case#2 with 24.2% and 14.0% respectively.

- Provide a superiorly clean environment for both patients and HCWs by combing the FFU with AIIR ventilation system Case#3. Add-on FFU (with HEPA filter) can play an important role in infection prevention in an AIIR.

The chosen ventilation system has an influence on the pollutant distribution and air flow pattern in the AIIR. Ventilation Case#3 is the improved system with less risk of infection from patients to HCWs. These findings are expected to provide important evidence that can aid in the development of design strategy for effective removal of airborne contamination in AIIRs.

Appendix A. Supplementary material

Supplementary data to this article can be found online at <https://doi.org/10.1016/j.applthermaleng.2018.11.023>.

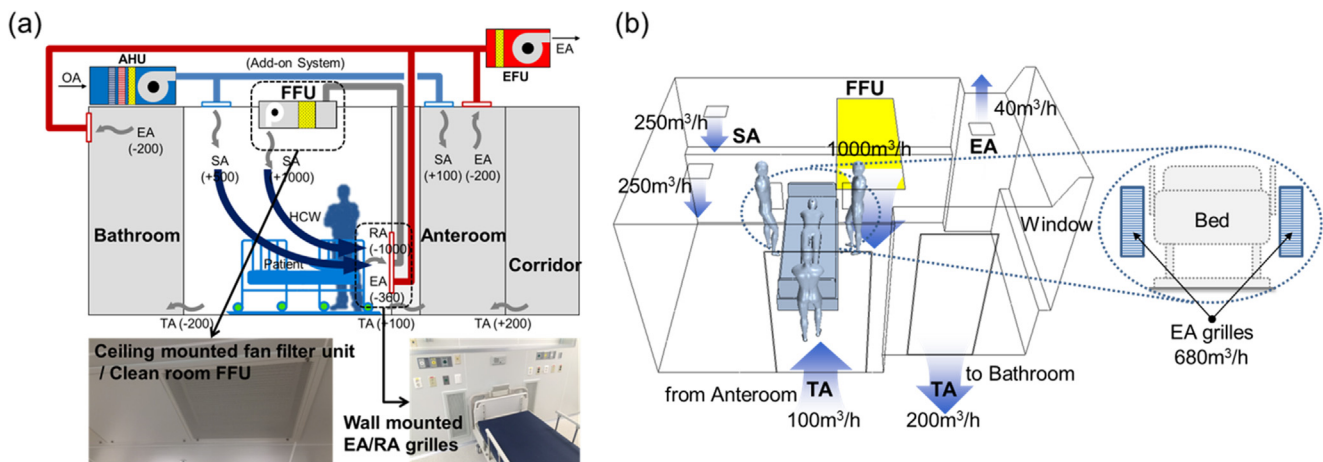


Fig. 10. Ventilation Case #3 with FFU; (a) Basic system configuration concept and (b) CFD modeling.

Table 7
Boundary conditions of ventilation Case #3 with FFU.

Case #3 w/FFU	Supply air	FFU	Exhaust/return air	Wall-mount / FFU
	Ceiling	Ceiling	Ceiling	Ceiling
	Airflow rate: 500 m ³ /h	Airflow rate: 1000 m ³ /h	Airflow rate: 40 m ³ /h	Airflow rate: 1360 m ³ /h
	V _{in} = 0.772 m/s	V _{in} = 1.852 m/s	V _{out} = 0.123 m/s	V _{out} = 1.717 m/s
	SA Diffuser (0.3 m × 0.3 m)	FFU outlet (0.15 m ²)	EA Grille (0.3 m × 0.3 m)	EA Grille (0.2 m × 0.55 m)
	2EA	1EA	1EA	2EA

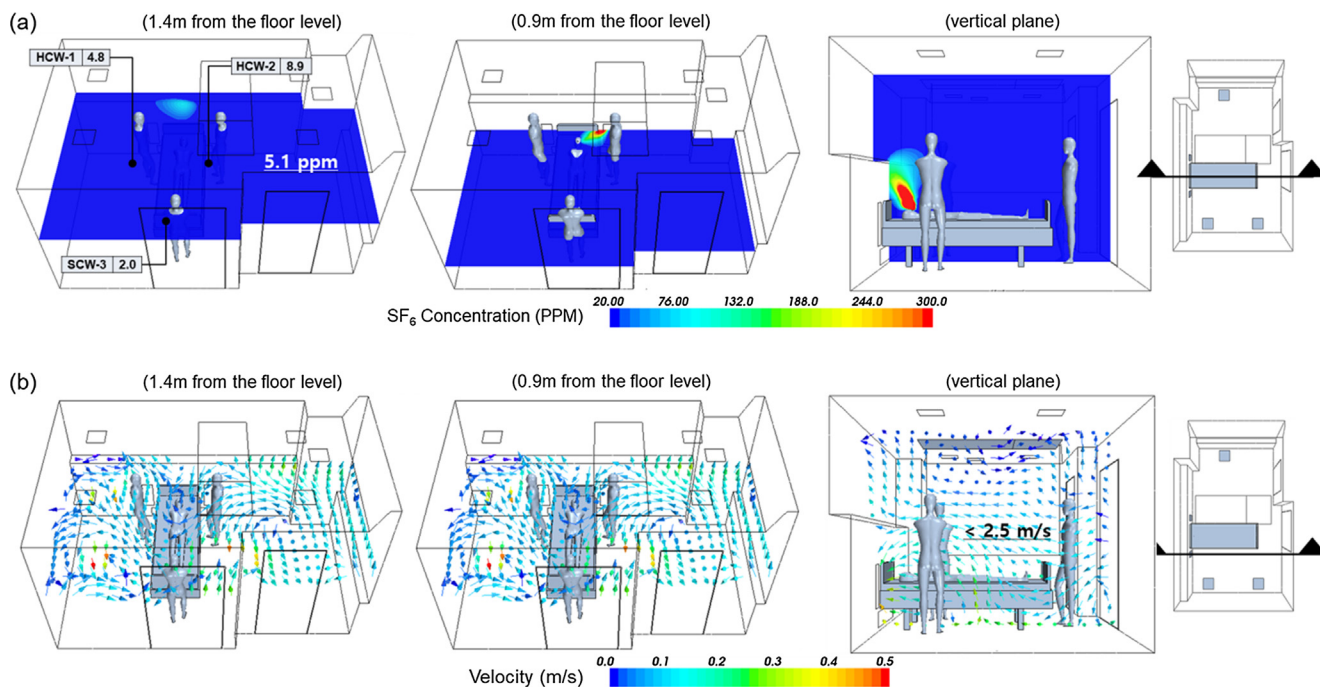


Fig. 11. Simulation results of ventilation Case #3 with FFU; (a) concentration profile of SF₆ and (b) velocity vector plot.

Table 8
The pollutant's exposure level of ventilation Case #3 with FFU.

	Mean SF ₆ concentration (ppm)		Percentage difference (%)
	Ventilation Case #3	Ventilation Case #3 w/FFU	(C _{v3-1} -C _{v3})/ C _{v3}
HCW-1 (1.4 m)	24.4	4.8	-80.3
HCW-2 (1.4 m)	21.2	8.9	-58.0
HCW-3 (1.4 m)	21.3	2.0	-90.6
Average of 1.4 m level	34.5	5.1	-85.2
Average of Room	34.8	7.1	-79.6

References

[1] T. Lim, J. Cho, B.S. Kim, Predictions and measurements of the stack effect on indoor airborne virus transmission in a high-rise hospital building, *Build. Environ.* 46 (2011) 2413–2424.
 [2] WHO, International travel and health. Geneva, Switzerland, World Health Organization, 2007.
 [3] K. Ha, A lesson learned from the MERS outbreak in South Korea in 2015, *J. Hosp. Infect.* 92 (2016) 232–234.
 [4] K.W. Mui, L.T. Wong, C.L. Wu, A.C.K. Lai, Numerical modeling of exhaled droplet nuclei dispersion and mixing in indoor environments, *J. Hazard. Mater.* 167 (2009) 736–744.
 [5] T. Lim, J. Cho, B.S. Kim, The predictions of infection risk of indoor airborne transmission of diseases in high-rise hospitals: tracer gas simulation, *Energy Build.* 42 (2010) 1172–1181.
 [6] Y. Tung, Y. Shih, S. Hu, Numerical study on the dispersion of airborne contaminants from an isolation room in the case of door opening, *Appl. Therm. Eng.* 29 (2009) 1544–1551.
 [7] S.H. Ho, L. Rosario, M.M. Rahman, Three-dimensional analysis for hospital operating room thermal comfort and contaminant removal, *Appl. Therm. Eng.* 29 (2009)

2080–2092.
 [8] N. Rice, A. Streifel, D. Vesley, An evaluation of hospital special-ventilation-room pressures, *Infect. Control Hosp. Epidemiol.* 22 (1) (2001) 19–23.
 [9] E. Bjorn, P.V. Nielsen, Dispersal of exhaled air and personal exposure in displacement ventilated rooms, *Indoor Air* 12 (3) (2002) 147–164.
 [10] J.M. Huang, S.M. Tsao, The influence of air motion on bacteria removal in negative pressure isolation rooms, *HVAC&R Res.* 11 (2005) 563–585.
 [11] H. Qian, Y. Li, P.V. Nielsen, C.E. Hyldgaard, Dispersion of exhalation pollutants in a two-bed hospital ward with a downward ventilation system, *Build. Environ.* 43 (3) (2008) 344–354.
 [12] Z. Rui, T. Guangbei, L. Jihong, Study on biological contaminant control strategies under different ventilation models in hospital operating room, *Build. Environ.* 43 (5) (2008) 793–803.
 [13] L. Morawska, Droplet fate in indoor environments, or can we prevent the spread of infection? *Indoor Air* 16 (5) (2006) 335–347.
 [14] Y. Li, S. Duan, I.T.S. Yu, T.W. Wong, Multi-zone modeling of probable SARS virus transmission by airflow between flats in Block E, Amoy Gardens, *Indoor Air* 15 (2) (2004) 96–111.
 [15] T.S. Yu Ignatius, Tze Wai Wong, Yuk Lan Chiu, Lee Nelson, Yuguo Li, Temporal-spatial analysis of severe acute respiratory syndrome among hospital inpatients, *Clin. Infect. Dis.* 40 (9) (2005) 1237–1243.
 [16] T. Hayashi, Y. Ishizu, S. Kato, S. Murakami, CFD analysis on characteristics of contaminated indoor air ventilation and its application in the evaluation of the effects of contaminant inhalation by a human occupant, *Build. Environ.* 37 (3) (2002) 219–230.
 [17] J.P. Abraham, B.D. Plourde, L.J. Vallez, Comprehensive review and study of buoyant air flow within positive-pressure hospital operating rooms, *Numer. Heat Transfer A* 72 (2018) 1–20.
 [18] K. Shirozu, T. Kai, H. Setoguchi, N. Ayagaki, S. Hoka, Effects of forced air warming on airflow around the operating table, *Anesthesiology* 128 (2018) 79–84.
 [19] ASHRAE, Ventilation of Health Care Facilities. Atlanta, GA, American Society of Heating Refrigerating and Air-Conditioning Engineers (ASHRAE standard 170-2013) (2013).
 [20] CDC, Guidelines for preventing the transmission of mycobacterium tuberculosis in health-care facilities 59(208) (1994), US Department of Health and Human Services, Public Health Services, Federal Register.
 [21] AIA, Guidelines for construction and equipment of hospital and medical facilities, The American Institute of Architect Press, Washington DC, 1987.

- [22] ASHRAE, HVAC Applications, American Society of Heating Refrigerating and Air-Conditioning Engineers (ASHRAE Handbook), Atlanta, GA, 2015.
- [23] K. Khankari, Airflow path matter; patient room HVAC, ASHRAE J. 58 (2016) 16–27.
- [24] J. Hang, Y. Li, R. Jin, The influence of human walking on the flow and airborne transmission in a six-bed isolation room: tracer gas simulation, Build. Environ. 77 (2014) 119–134.
- [25] F.J. Offermann, A. Eagan, A.C. Offermann, S.S. Subhash, S.L. Miller, L.J. Radonovich, Potential airborne pathogen transmission in a hospital with and without surge control ventilation system modifications, Build. Environ. 106 (2016) 175–180.
- [26] ASHRAE, Method of testing general ventilation air-cleaning devices for removal efficiency by particle size, American Society of Heating Refrigerating and Air-Conditioning Engineers (ASHRAE standard 52.2), Atlanta, GA, 2007.
- [27] K.W.D. Cheong, S.Y. Phua, Development of ventilation design strategy for effective removal of pollutant in the isolation room of a hospital, Build. Environ. 41 (2006) 1161–1170.
- [28] ASHRAE, Thermal environmental conditions for human occupancy, American Society of Heating Refrigerating and Air-Conditioning Engineers (ASHRAE standard 55), Atlanta, GA, 2010.